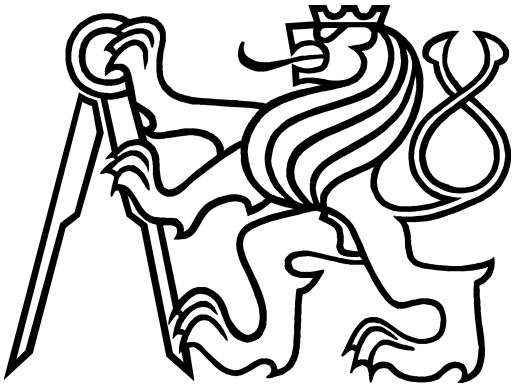

LULEÅ
UNIVERSITY
OF TECHNOLOGY

Misael Eduardo Bejarano Jiménez

Multivariable control for surface deformation.

Thesis submitted in partial fulfillment of the requirements for the degree of Master of Science in Technology

Prague May 29, 2008

Supervisors:

Martin Hromčik
Czech Technical University

Thomas Gustafsson
Luleå University of Technology

Instructor:

Martin Hromčik
Czech Technical University

Preface

In the following a *LQG* control approach in the framework of disturbance rejection is presented. Modeling of a system consisting on a rod, for two materials Aluminium and Acrylic, acted by piezo transducers is also addressed by means of a Finite Element analysis and its further exporting to MATLAB. Selection of a proper confiuration of piezo actuators and perifericals is stated as well.

I would like to deeply thank all my teachers in the Space Master course for all his patience and good will.

The number of books will grow continually, and one can predict that a time will come when it will be almost as difficult to learn anything from books as from the direct study of the whole universe. It will be almost as convenient to search for some bit of truth concealed in nature as it will be to find it hidden away in an immense multitude of bound volumes.

Denis Diderot

Prague, May 29, 2008

Misael Eduardo Bejarano Jimenez

Declaration

I hereby declare that I have completed this master thesis independently and that I have listed all the literature and publications used. I have no objection to usage of this work in compliance with the act §60 No. 121/2000Sb. (copyright law), and with the rights connected with the copyright act including the changes in the act.

In Prague, May 29, 2008 .....

CZECH TECHNICAL UNIVERSITY OF TECHNOLOGY IN PRAGUE

ABSTRACT OF THE MASTER'S THESIS

Author:	Misael Eduardo Bejarano Jimenez		
Title of the thesis:	Spatially distributed control for surface deformation		
Date:	May 29, 2008	**Number of pages:**	41
Faculty:	Electrical Engineering		
Department:	Control Engineering		
Supervisor:	Martin Hromcik (CVUT) and Thomas Gustafsson (LTU)		
Instructor:	Martin Hromcik		

This work addresses the modeling (in FEMLAB) and multivariable *LQG* control configuration design for the damping of vibration over to different scenarios, first an acrylic rod, and then in an aluminium one. A good review of Finite Element Method is provided as well as issues related to the FEMLAB and its link environment to MATLAB.

Keywords: *LQG*, Multivariable, FEM, Vibration, FEMLAB.

Contents

Chapter 1

Introduction

Nowadays space imagining is facing a wide range of problems looking forward to make more accurate and more powerful observations in the sake of space exploration and research. The duo sensor-actuator is the starting point for building space-capable probes task that, even when performed on Earth has to be thought for an extreme environment as the one found out of the planet.

Space environment represent a *colorful* source of disturbances for almost every subsystem in a spacecraft namely satellite, shuttle or more *oriented* device as could be a telescope is affected by them. Electronic parts are normally affected by parasitic currents due that ionization in metal structures used for voltage reference, materials in general are subject of vacuum effects as well as micrometeorites, mechanical structures and optical elements work under thermic and vibrational non desired conditions and so forth with the other subsystems in the space probe.

Therein disturbances are, as always, an issue to consider and their effects are meant to be avoided as much as possible being this a priority regardless the nature of the mission's aim simply because they introduce a non

expected behavior in the system.

This work is mainly inspired by the adaptive optics and the control of spatially distributed systems. As a future aim is to counteract and correct deformation caused by both environment (atmospheric interference, thermic effects) and mechanical (vibrations and deformations) disturbances that corrupts the surface of the optical filter in an x-ray sensor that has been probed in medicine and scientific imaging with more than good results, for future earth and space-based imaging, by means of using a large piezo patch net as sensor-actuator device coordinated by a decentralized spatially distributed control.

In the following the design of a control system for disturbance rejection for two models of a plant consisting of a rod and piezo patches as actuators is developed based on LQG theory.

1.1 Objectives

To provide a stable robust control for the disturbance rejection on an aluminium rod as a first approach to the control of a spatially distributed control problem as it could be the the surface deformation of a mirror or the optical filter in a sensor. This work is mainly inspired by adaptive optics and the control of spatially distributed systems and has as primary objectives:

1. To develop an accurate model to the plant rod-piezo actuator.
2. To design a control system for a rod actioned by piezo patches with emphasis in disturbance rejection. This sugests that integration may be needed.

3. To define an optimal approach for the already defined problem. We will discuss about two possibilities that solve our necessities which are a LQG control.

4. The control input shall not be influenced by the measurement noise.

Chapter 2

Related Work

The aim of the following is to provide an overview of the knowledge needed to design the control configuration for the proposed plant. First to explain what is the Finite Element Method, then how does it work and how it was used to generate two models of the plant under two different sets of specifications and assumtions. Second to explaint the nature of the actuator and how it will be used in a possible real implementation of the present work. A selection of the most suitable piezo patch as well as power source and PC interface is also provided. And third to comment about the theory behind the *LQG* control.

2.1 The Finite Element Method *FEM*

The FEM approximates the solution of a *PDE* problem by discretizating it. This method introduces *shape functions*[1] that describe the possible forms

[1]This shapes are defined by the order and type of the analysis for example one can say a cubic or quadratic Lagrange element or Hermite element. To see the advantages of each one of this please refer to (4)

of solution of the original *PDE* problem.

FEM start point is a mesh. A mesh is basically the partition of the geometry into small units of a simple shape. In a $2D$ problem [2] normally this ellements are triangles. The sides of the triangles are called mesh edges, and their corners are mesh vertices. A mesh edge must not contain mesh vertices in its interior. Similarly, the boundaries defined in the geometry are partitioned (approximately) into mesh edges (so-called boundary elements) that must conform with the triangles if there is an adjacent subdomain. There might also be isolated points in the geometry. These also become mesh vertices.

Once you have a mesh, you can introduce approximations to the dependent variables. For this discussion, we will concentrate on the case of a single variable, u. The idea is to approximate u with a function that you can describe with a finite number of parameters, the so-called degrees of freedom (DOF). Inserting this approximation into the weak form of the equation generates a system of equations for the degrees of freedom.

Then a finite element set is generated based in the DOF and the order and type of element. This set is a set of equations that satisfy for each element in the mesh the conditions impoused by the type of element. Next the method discretize this set for boundaries, points and subdomines in the geometry[3].

2.1.1 Strain-Displacement Relationship

It is possible to completly describe the strain conditions in a point with deformations components u,v,w in 3D and their derivatives. The shear

[2] As it is our case. This will be discussed in section 2.3.2.

[3] A subdomine is each part of the final geometry generated while modeling

strain tensor can be expresed as ϵ_{xy}, ϵ_{xz}, ϵ_{yz}. Then by following the small-displasment assumtion the normal strain components and the shear strain components are given from the deformation as follows:

$$\epsilon_x = \frac{\partial u}{\partial x} \tag{2.1}$$

$$\epsilon_y = \frac{\partial v}{\partial y} \tag{2.2}$$

$$\epsilon_z = \frac{\partial w}{\partial z} \tag{2.3}$$

$$\epsilon_{xy} = \frac{1}{2}(\frac{\partial u}{\partial y} + \frac{\partial v}{\partial x}) \tag{2.4}$$

$$\epsilon_{xz} = \frac{1}{2}(\frac{\partial u}{\partial z} + \frac{\partial w}{\partial x}) \tag{2.5}$$

$$\epsilon_{yz} = \frac{1}{2}(\frac{\partial v}{\partial z} + \frac{\partial w}{\partial y}) \tag{2.6}$$

Then the simetric strain tensor ϵ is defined as:

$$\begin{bmatrix} \epsilon_x & \epsilon_{xy} & \epsilon_{xz} \\ \epsilon_{yx} & \epsilon_y & \epsilon_{yz} \\ \epsilon_{zx} & \epsilon_{zy} & \epsilon_z \end{bmatrix}$$

2.1.2 Strees-Strain Relationship

The stress in a material is described by the symmetric stress tensor:

$$\sigma = \begin{bmatrix} \sigma_x & \tau_{xy} & \tau_{xz} \\ \tau_{yx} & \sigma_y & \tau_{yz} \\ \tau_{zx} & \tau_{zy} & \sigma_z \end{bmatrix} \tag{2.7}$$

Where σ_i is the normal strees, τ_{ij} shear strees and if symetry is used τ_{ij} equals τ_{ji}. The strees-strain relation is defined as:

$$\sigma = D\epsilon \tag{2.8}$$

Where D is a 6x6 elasticity matrix and:

$$\sigma = \begin{bmatrix} \sigma_x \\ \sigma_y \\ \sigma_z \\ \sigma_{xy} \\ \sigma_{xz} \\ \sigma_{yz} \end{bmatrix} \tag{2.9}$$

And

$$\epsilon = \begin{bmatrix} \epsilon_x \\ \epsilon_y \\ \epsilon_z \\ \epsilon_{xy} \\ \epsilon_{xz} \\ \epsilon_{yz} \end{bmatrix} \tag{2.10}$$

D is defined diferently for Isotropic, Orthotropic and Anisotropic[4] materials. For Isotropic material D is defined as follows:

[4]When Isotropic, materials have the same properties in all cristallographic directions, when Orthotropic, the properties are different in different directions and when Anisotropic, properties can changes suddendly in the same direction as is the case of composite materials.

$$D = \frac{E}{(1+v)(1-2v)} \begin{bmatrix} 1-v & v & v & 0 & 0 & 0 \\ v & 1-v & v & 0 & 0 & 0 \\ v & v & 1-v & 0 & 0 & 0 \\ 0 & 0 & 0 & \frac{1-2v}{2} & 0 & 0 \\ 0 & 0 & 0 & 0 & \frac{1-2v}{2} & 0 \\ 0 & 0 & 0 & 0 & 0 & \frac{1-2v}{2} \end{bmatrix} \tag{2.11}$$

Where E denotes *Young's module* or elasticity module, and v denotes the *Poisson's ratio* which defines contration in the perpendicular direction. Normally, for simplicity $D^{-}1$ is used for calculation because it is more basic.

2.1.3 The equilibrium equation and it implementation in 3D

The equilibrium equation in 3D is defined as:

$$-\frac{\partial \sigma_x}{\partial x} - \frac{\partial \tau_{xy}}{\partial y} - \frac{\partial \tau_{xz}}{\partial z} = F_x \tag{2.12}$$

$$-\frac{\partial \tau_{xy}}{\partial x} - \frac{\partial \sigma_y}{\partial y} - \frac{\partial \tau_{yz}}{\partial z} = F_y \tag{2.13}$$

$$-\frac{\partial \tau_{xy}}{\partial x} - \frac{\partial \tau_{zy}}{\partial y} - \frac{\partial \sigma_z}{\partial z} = F_z \tag{2.14}$$

Or using compact notation:

$$-\nabla \sigma = F \tag{2.15}$$

Where F denotes the volume forces (body forces) and σ is the strees tensor. Substituting the Strees-Strain and Strain-displasment in the above equation results in Navier's equation expresed in displasment, this is like follows:

$$-\nabla(c\nabla u) = F \tag{2.16}$$

2.2 Piezo Patch

The development of self-correcting, adaptive systems is receiving more and more attention in modern industrial research. Structures using "smart materials" which integrate sensor and actuator functions are taking on growing importance in this field. These systems are designed to detect and react to changes in their operating environment, like impact, pressure or bending forces.

With a long history as adaptive materials, piezo actuators have been especially popular for the monitoring and active damping of high-frequency vibration due that its composite fiber technologies that transform electrical to mechanical energy and vice versa make them ideal for prototyping and research.

The *piezoelectric effect* was discovered in 1880 by Jacques and Pierre Curie when observed that piezo electric materials [5] can change its form when an electric potential is applied to them, in addition when pressure acts over this kind of materials an electric current proportional to the motion is generated, this phenomena is known as the *inverse piezoelectric effect*.

[5] Named like that once that the already mentioned effect were discovered i.e. Aluminum nitride, Apatite, Lead scandium tantalate, Potassium sodium tartrate, Quartz and so forth.

Piezo patches, or piezo actuators, can be used in different configurations when attached to a substrate as:

- Sensor: Minute deformations in the substrate, within the influence area of the device, cause displacements in the patch transducer that originates an electric current proportional to the motion, see Figure 2.2. One can take advantage of this using more than one patch.

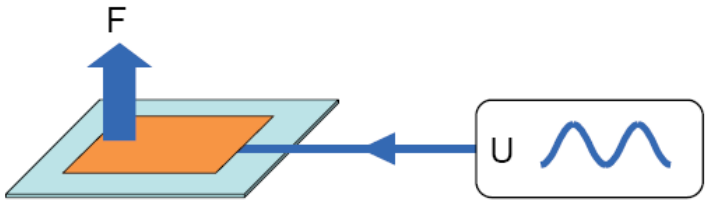

Figure 2.1: Piezo patch used as an Actuator. When voltage is supplied the patch reacts changing it form, when attached to a substrate it acts as a bender. (4)

- Actuator: Using the inverse piezo effect the patch, once that a voltage is supplied, it acts as a bender, see Figure 2.1, by means of generating a lateral force that it transmitted to the substrate.
- Sensor-Actuator: When multilayered the sensor signal can be used as power supply for the same module where it is feedback with a face shift. This mode depends on the supplier. Used widely in adaptronics.
- Power supply: Provide power for low-consumption devices making the develop of autonomous systems possible.

It is worth to mention that adaptive materials are used in particular for vibration reduction in vehicles, and their use in mechanical engineering is growing. Piezo transducers are suitable for active and adaptive systems. Embedded in a control loop they can reduce vibrations and control strutures in the nanometer range.

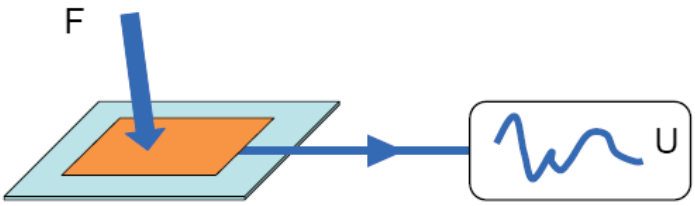

Figure 2.2: Piezo patch used as a sensor. A source is applied in the surface in form of impact, pressure or bending, this generates a current proportional to the motion that source causes to the patch. (4)

To operate a high-precision, high-dynamics positions, a low noise, broad band amplifier is required. Active vibration damping requires a fast control with sufficient bandwidth for close-coupling the generated force to the structural mass to be damped. PI also manufactures the power source E-413.D2 which is capable of provide the voltage [6] necessary for providing precision control in open loop for piezo shear and bender actuators in both static and dynamic operation.

As a consideration for possible practical implementation one might think about the fact that the E-413.D2 module is capable of being controlled by PC or μC through D/A converter. It comes with an optional National Instruments LabVIEW driver which is compatible with the GCS making "easy" the operation of the overall system.

[6] -100V to 400V @ 50W

Table 2.1: System Configuration for Vibration Control.

Piezo Actuator	**Power Source**
P-876.A15	E-413.D2
Primary Device	

2.3 Modeling

Two models were developed in the present work. One, the so called *push-up* approach was developed as a simplification of the problem but, as it is developed in the following sections, the assumptions made within the modeling process are not quite useful in reality thats the reason for developing a second model, the so called *realistic* approach which corrects the wrong ideas and give a more realistic, as its name indicates, model of the problem including as well mechanical specifications of the piezo patch.

Each one of the models were generated based on a *FEM* analysis under FEMLAB environment, specifically using the module of static structural analysis with the mechanical properties listed in Table 2.2.

Using *FEMLAB* a model can be generated by specifying a *FEM* problem. This is described in the following steps:

1. A geometry has to be constructed. *FEMLAB* provides an environment in which is possible to draw similar to those one can find in AUTOCAD or any other CAD software including of course the possible importing of IGES, STEPS and some other standards in mechanical drawing. Of course the most common is that the geometry will be composed by sub-geometries which is our case.

2. Setting the analysis by means of declaring constants; that for both analysis were the applied force, boundary conditions; that for our case

were that the extremes of the rod could not move, declaring the forces and where and how they act and the mechanical properties for the elements in the analysis (Table 2.2). For a detailed description about how and where the forces were thought to act see the description of the approaches.

3. Mesh the geometry. For more information on this regard refer to previous sections on *FEM* analysis.

4. Specifying and solving the *FEM* problem. In this regard the analysis used was static because our main interest was to calculate the deflection of the rod. For more on this refer to previous sections on *FEM* analysis.

5. Exporting the solution to MATLAB. For doing this input and output variables are declared as well as the order reduction degree that is desired. One must remember that exporting the "complete" model means that the exported solution will have as much as three times the *DOF*.

Once the solver acquired the solution for the *FEM* problem and exported to MATLAB on a space state form the analysis and design of the control structure [7] may begin.

Next the approaches developed in this work are explained.

[7] One must make a distinction on the control *structure* and control *configuration*. Control structure (or strategy) refers to the structural decisions included in the design of a control system and control configuration refers only to the structuring (decomposition) of the K controller itself (5).

Table 2.2: Mechanical Specifications of piezo patch and aluminium rod used in *FEMLAB* modeling

Specification	**Pushed-up Rod**	**Realistic Rod**	**Piezo Patch**
Young's Module (E) $[Pa]$	2e11	55e9	30e9
Poisson's Ratio (ν) []	0.33	0.35	0.25
Density (ρ) $[Kg/m^3]$	7850	1190	2450
Thickness $[m]$	xxxx	0.035	0.035

2.3.1 The push-up approach

It consist basically on the simplification of the force caused by the surface traction that the piezo patch induces in the subtract, in this case an *acrylic rod*, by means of thinking about it as a localized force. On Figure 2.3 one can see the geometry that was made for this issues, there are 9 points indicating the place in which the forces were assumed to be. In this approach the sensors were assumed to be at the same place than the actuators. The magnitude of the force was some how arbitrary but always the idea of *real world* in the sens of that the force's magnitude should be enough to deform the rod but not too high to break it was kept. One can see the deformation of the geometry in Figure 2.4.

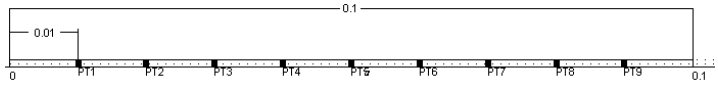

Figure 2.3: Mechanical drawing of the geometry used to model the so called *push-up* approach to the piezo patch problem. It is an extruded square of 5mm x 5mm x 10cm. Units in the figure are in meters $[m]$ for consistence with the analysis performed.

The magnitude of the forces acting on the acrylic rod was chosen to be between $50N$ and $75N$ due that the fragile structure of the material. This assumption was made based on experimental results of tension tests. Their

direction was inserted one positive and one negative according to the y axis. This convention explains the deformed shaped showed in 2.4.

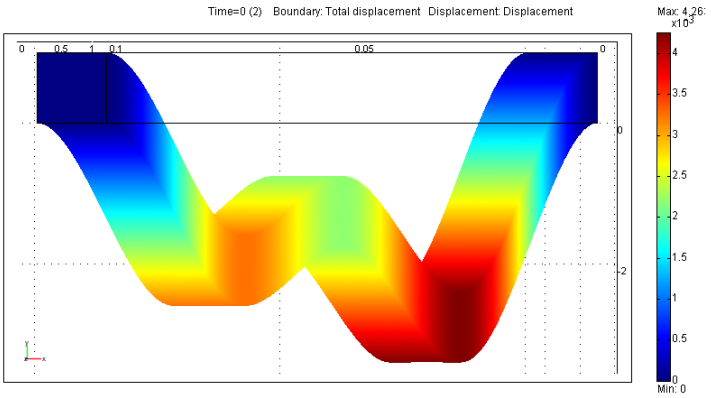

Figure 2.4: Deformation plot result of the action of 9 localized forces over an acrylic rod used in the *push-up* approach to the piezo patch problem. One can see a colored scale of the deformation with units in m

2.3.2 The realistic approach

In the *realistic approach* the simplification of the traction force in the (in this case) *aluminium rod* was replaced by a more accurate idea that is the consideration of it as result of two forces acting over the longitude of the piezo patch contact with the substrate. This generate a response observed by (2). The system consists on 3 piezo patches (for specifications refer to the section on Piezo Patches) distributed and attached along the rod in the configuration shown in Figure 2.5.

In this approach the sensors were assumed to be the patches them self, this can be done due that the piezo patch model selected can be wired for serving both porpoises without lost of accuracy, so, 6 points, 2for each patch, were introduced in the the model for setting the output of the simulation and of course output variables for the control model. This points were placed inside the effect area of the patch (4).

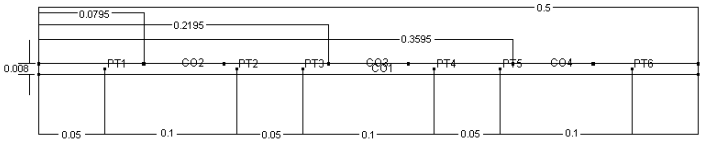

Figure 2.5: Mechanical drawing of the geometry used to model the so called *realistic* approach to the piezo patch problem. It is a rod of 0.5m x 8mm. **Thickness is 3.5cm**. Units in the figure are in meters $[m]$ for consistence with the analysis performed.

It is important to notice that the forces for this model were not assumed but taken from the data sheet of the piezo patch selected. This force corresponds to $750N$ as a maximum and it is generated in the borders of the patch, it is, in fact, known as lateral contraction force. Due to this fact the forces acting on the aluminium rod were placed on the borders of each patch and its influence were calculated as force over the length in z direction (thickness) of the patch.

One can see that the deformed shape showed in Figure 2.6 exhibits a more coupled behavior than the one for the *push-up* approach. This fact is due that the first model was generated in a $3D$ environment (not in $2D$ as the second) fact that do not allow the designer to have a *detailed* analysis of the movement in the sense of lost of accuracy and coupling with the third axis z.

2.4 H_2 Control

The H_2 control problem consists of stabilizing the control system while minimizing the H_2 norm of its transfer function (3). This is accomplish by finding the stabilizing controller $\mathbf{K}$ wich minimizes

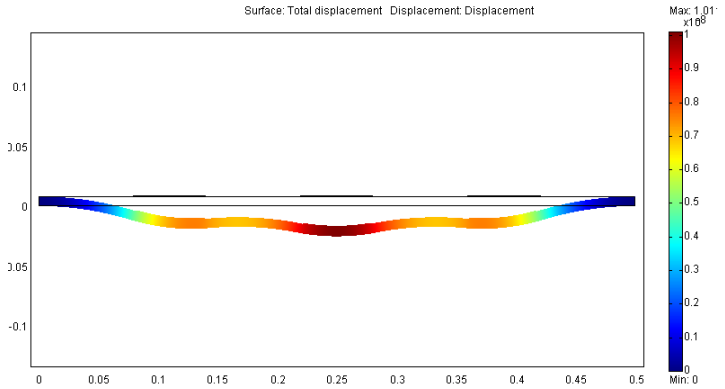

Figure 2.6: Deformation plot result of the lateral contracting force acting over the geometry used in the *realistic* approach to the piezo patch problem. One can see a colored scale with units in m

$$\|F(s)\|_2 = \sqrt{\frac{1}{2\pi}\int_{-\infty}^{\infty} tr\left[F(j\omega)F(j\omega)^H\right] d\omega} \tag{2.17}$$

$$F \triangleq F_l(P, K) \tag{2.18}$$

For a particular problem the generalized plant P will include the plant model, the interconnection structure, and the designer-specified weighting functions (5). Among several interpretations that the H_2 control has the following stochastic interpretation also holds. Supouse that in the general control configuration (see 2.7) the exogenous input w is with noise of unity intensity:

$$Ew(t)w(t)^T = I\delta(t-\tau) \tag{2.19}$$

The expected error z is given by:

$$E = \lim_{T\to\infty} \frac{1}{2T}\int_{-T}^{T} z(t)^T z(t) dt \tag{2.20}$$

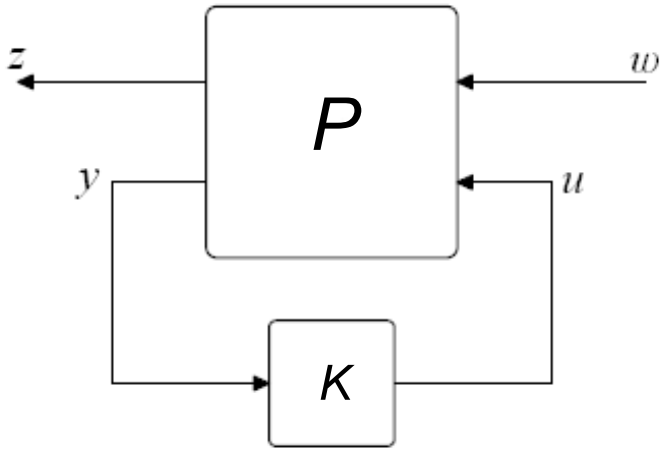

Figure 2.7: General Control Configuration. The signals are: u the control variables, v the measured variables, w the exogenous signals such disturbances and commands and z the so-called error signals that are to be minimized in some sense to meet the control abjective. (4)

$$= trEz(t)z(t)^T \tag{2.21}$$

$$= \frac{1}{2\pi}\int_{-\infty}^{\infty} tr\left[F(j\omega)F(j\omega)^H\right]d\omega \tag{2.22}$$

$$= \|F\|_2^2 = \|F_l(P,K)\|_2^2 \tag{2.23}$$

The closed-loop transfer function form w to z is given by the LFT

$$z = F_l(P,K)w \tag{2.24}$$

where

$$F_l(P,K) = P_{11} + P_{12}K(I - P22K)^{-1}P_{21} \tag{2.25}$$

Thus, by minimizing the H_2 norm, the output (or error) power of the generalized system, due to a unit intensity white noise input, is minimized (by Parseval's theorem); this is the minimization of the root-mean-square (rms) value of z.

2.4.1 LQG: A special H_2 optimal controller

An important special case of H_2 optimal control is the LQG controller. Assuming that the dynamics of the system are linear and known, and that the input and process noises are available and stochastic with known statistical properties, then one can concider the plant model:

$$\dot{x} = Ax + Bu + w_d \tag{2.26}$$

$$y = Cx + Du + w_n \tag{2.27}$$

Where w_d,w_n are the disturbance (proces noise) and measurement noise respectively, which are usually assumed to be uncorrelated zero-mean Gaussian with constant power spectral density matrices W and V respectively. Where

$$Ew_d(t)w_d(\tau)^T = W\delta(t-\tau) \tag{2.28}$$

$$Ew_n(t)w_n(\tau)^T = V\delta(t-\tau) \tag{2.29}$$

$$Ew_n(t)w_d(\tau)^T = Ew_d(t)w_n(\tau)^T = 0 \tag{2.30}$$

Where E denotes expectation and $\delta(t-\tau)$ is the delta function. The LQG control problem then is to find the optimal control $u(t)$ that minimize the cost function:

$$J = E \lim_{T \to \infty} \frac{1}{T} \int_0^T [x^T Q x + u^T R u] dt \tag{2.31}$$

Where Q and R are weighting matrices such that $Q = Q^T \geq 0$ and $R = R^T \geq 0$.

The solution to the LQG problem is known as the separation principle (certainty equivalence principle) and consists in first finding the optimal controller for a deterministic linear quadratic regulator LQR.[8] It happens that the solution to this problem is rather elegant and simple and it can be written as a simple state feedbacl law:

$$u(t) = -K_r x(t) \tag{2.32}$$

With $-K_r$ as a constant matrix independent of W and V. Note that under this control law it is required that $x(t)$ is available for feedback, which generally it is not the case. To overcome this difficulty one can determine an optimal state estimate $\hat{x}$ of the state x. This is the second step in the design of a LQG and it is accomplished by designing a Kalman filter that generates the optimal state estimate $\hat{x}$ independently of Q and R. Then the required solution to the LQG problem is then found by replacing x by $\hat{x}$ to give $u(t) = -K_r \hat{x}$. See 2.8

LQR problem

The LQR problem has the advantage that all the states are known, the problem is to find the initial value $u(0)$ for a system $\dot{\hat{x}} = Ax + Bu$ with a

[8] That in a practical approuch is the LQG problem without w_d and w_n

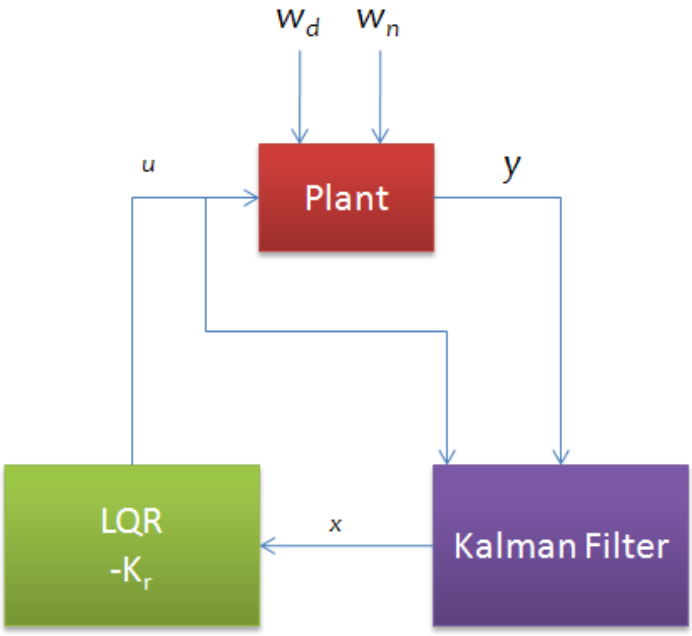

Figure 2.8: The separation theorem.

non trivial solution which takes the system to the zero state in an optimal manner by means of minimizing the cost function:

$$J_r = \int_0^\infty (x(t)^T Q x(t) + u(t)^T R u(t) dt) \tag{2.33}$$

Where the optimal solution for any initial state is $u(t) = -K_r x(t)$ with

$$-K_r = R^{-1} B^T X \tag{2.34}$$

and $X = X^T \geq 0$ as the unique positive semi-definite solution of the ARE

$$A^T X + XA - XBR^{-1}B^T X + Q = 0 \tag{2.35}$$

The Kalman Filter

The Kalman filter has the structure of an observer or state stimator 2.9. That allows us to reconstruct usable state and disturbance estimates from the measurements, enabling us to solve the measurement feedback synthesis problem, which is our main interest. With:

$$\dot{\hat{x}} = A\hat{x} + Bu + K_f(y - C\hat{x}) \tag{2.36}$$

Where K_f is meant to be optimally chosen by minimizing $E = [x - \hat{x}]^T[x - \hat{x}]$ thrugh

$$K_f = YC^TV^{-1} \tag{2.37}$$

With $Y = Y^T \geq 0$ as the unique positive semi-definite solution of the ARE:

$$YA^T + YA - YC^TV^{-1}CY + W = 0 \tag{2.38}$$

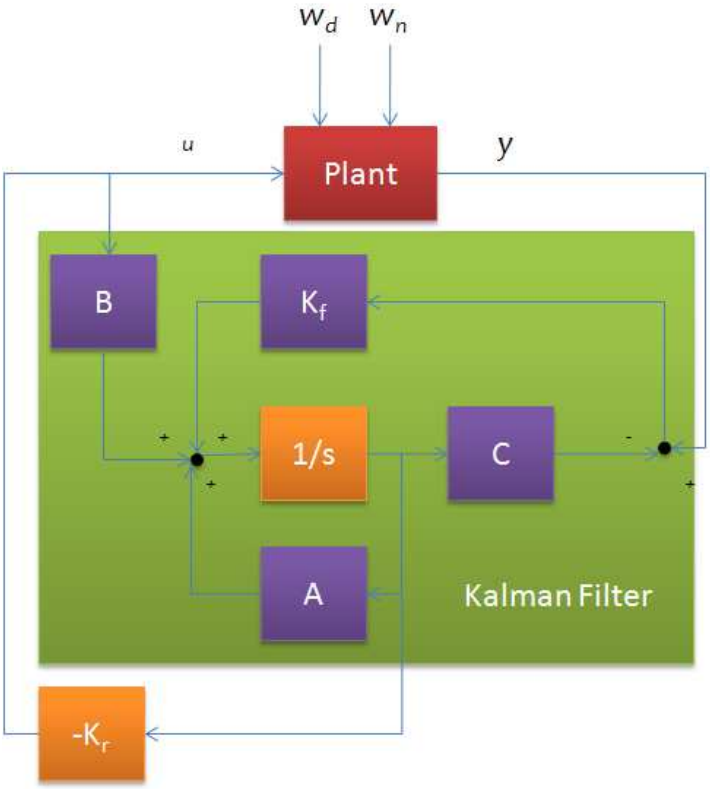

Figure 2.9: The LQG controller with noisy plant.

Chapter 3

Results

The control configuration followed in this work is mainly multivariable feedback LQG, explained earlier on the section about H_2 control, which has been probed its effectiveness in a lot of areas of application from chemical industry to aerospace applications. In the following the results of the control design and test for both approaches are showed and explained. Also a PI controller for the *push-up* scenario is briefly touched as well as the MATLAB virtual reality model used for visualizing the simulations.

It is worth to mention that all the controllers (at least those LQG) were synthesized by giving a weight to the W and V matrices according to the next procedure which is performed by a MATLAB script that can be seen in the Appendix A.

$$\mathrm{J}_{LQG} = \lim_{T\to\infty} E\left\{\int_0^T |x'u'|\, W\, |xu|'\, dt\right\} \tag{3.1}$$

Where:

$$W = \begin{bmatrix} Q & 0 \\ 0 & R \end{bmatrix} \tag{3.2}$$

Subject to the dynamics

$$dxdt = Ax + Bu + Xi \tag{3.3}$$

$$y = Cx + Du + Th \tag{3.4}$$

Where Xi and Th are white uncorrelated noises that together form the noise weighting matrix:

$$W = \begin{bmatrix} Xi & 0 \\ 0 & Th \end{bmatrix} \tag{3.5}$$

For more details on what is Q, R, Xi and Th refer to Section 2.4.1.

3.0.2 The *push-up* approach

As stated earlier in the present, the LQG strategy was chosen to be the guide for developing a disturbance rejection control configuration. Although for the *push-up* approach to the piezo patch problem it was also developed, not with the same emphasis, a PI controller just for the sake of comparing Nominal and Robust performance for the two approaches.

LQG control

In Table 3.1 one can see eigenvalues of the plant (with dominant pole in -10.71) without any control action and under effect of white noise going directly to the states, its deformation, due to this vibrational disturbance, in terms of the positions of each of the 9 points that where used as origin for the localized force and the sensor location itself can be seen in Figure 3.1.

Table 3.1: Eigenvalues for the plant on the *push-up* approach.

Plan Eigenvalues			
-1.2223e7	-5.3120e5	-1.4337e4	-2.1940e3
-1.2200e7	-1.7705e5	-1.1702e4	-9.3418e2
-1.0788e7	-1.2020e5	-1.1233e4	-5.9748e2
-1.0763e7	-8.9791e4	-8.8361e3	-5.7873e2
-7.3659e6	-4.3354e4	-5.6825e3	-4.9055e2
-7.3471e6	-2.0049e4	-4.8907e3	-4.4887e2
-6.5883e5	-1.9720e4	-4.5761e3	-8.5828e1
-6.3197e5	-1.5491e4	-4.0908e3	**-1.0708e+001**

A *LQG* controller was synthesized with parameters listed in Table 3.2 in consistence with the objectives listed in Section 1.1[1].

In the Table 3.3 the eigenvalues for the *push-up* feedback system performing under the same conditions, this means, with white noise acting directly on the states with dominant pole placed in the same place than in the plant without controller, just that in this case the multiplicity of poles in this place is of 17. This fact *robustifies* the system against some perturbations, never the less is worth saying that in the present analysis robust

[1]One can perform the synthesis easily by just making a copy-paste of the provided code using the already listed parameters. Control structure is not included due to space and relevance.

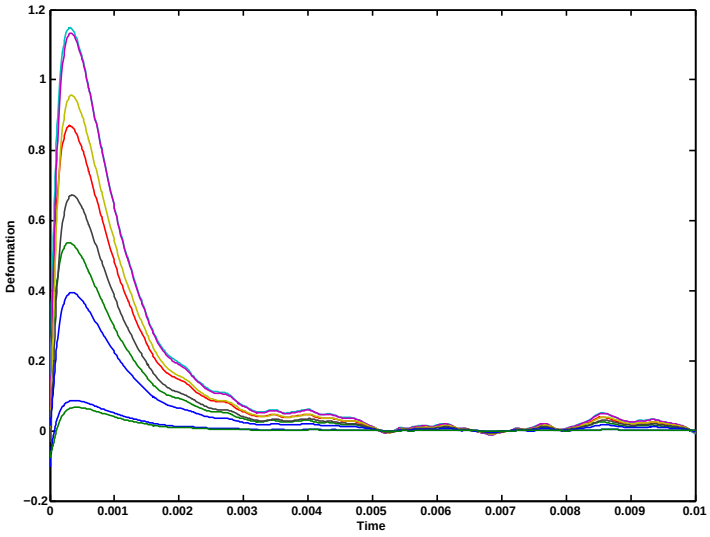

Figure 3.1: Response of the *Push-up* plant for a random initial state with white noise acting on the states. Unites where scaled to millimeters.

Table 3.2: Specifications for *push-up LQG* synthesis.

Weight on	**Value**
Q	1
R	1e-5
Xi	1e-5
Th	1

performance can not be probed for any design due that uncertainty was not consider explicitly. Numbers showed in a () denote multiplicity, as already stated. In figures 3.2 and 3.3 one can see the control effort in the time domain for this approach.

Table 3.3: Eigenvalues for the controller-plant feedback on the *push-up* approach.

Feedback Eigenvalues			
-2.4298e8(2)	-5.0184e6(2)	-1.0172e4 -9.0933e3i	-1.0095e3
-1.9554e8(2)	-2.7115e6(2)	-6.3103e3	-1.0046e3
-1.4491e8(2)	-1.3207e6(4)	-3.4429e3	-1.0027e3
-1.0337e8(2)	-5.9333e5(4)	-1.3006e3	-1.0017e3
-7.2875e7(2)	-2.1711e5(4)	-1.1881e3	-1.0010e3
-1.2617e7(2)	-5.5859e4(2)	-1.0450e3	**-1.0008e3(17)**
-8.5957e7(2)	-1.0172e4 +9.0933e3i	-1.0182e3	

One can see in figures 3.4 and 3.5 the behavior of the feedback loop in time domain.

PI Control

As a brief remark it is included a PI controller for the *push-up* approach. One can imagine clearly from the Figures 3.6 and 3.7 that the controller satisfies nominal performance in a certain degree, this is mainly observed form the feedback behavior in Figure 3.7.

This design was neglected for further analysis due that the gain required for its operation as it is showed in the already mentioned figures is very high, in the order of the 10000. Obviously this is not something that can be achieved by a piezo-transducer available in the market. This controller

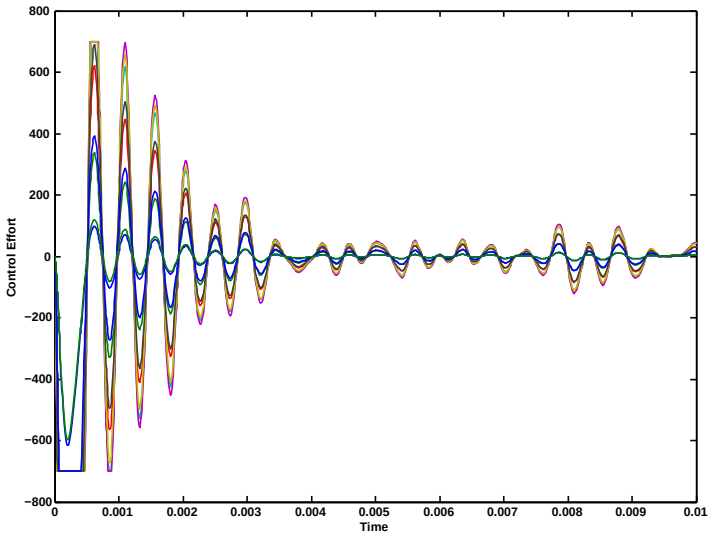

Figure 3.2: Control effort for the LQG synthesized for the push-up system. One can notice the assumed saturation limits of $700N$ of the actuators in the early stages of control action.

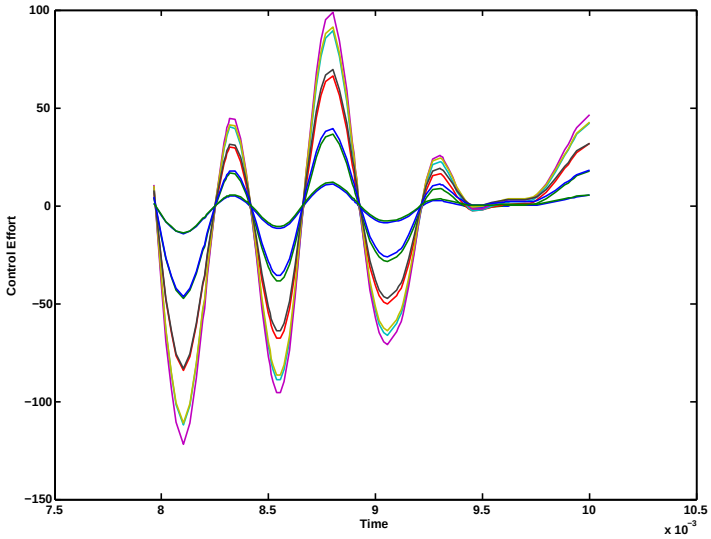

Figure 3.3: Control effort in steady state for the LQG synthesized for the push-up system.

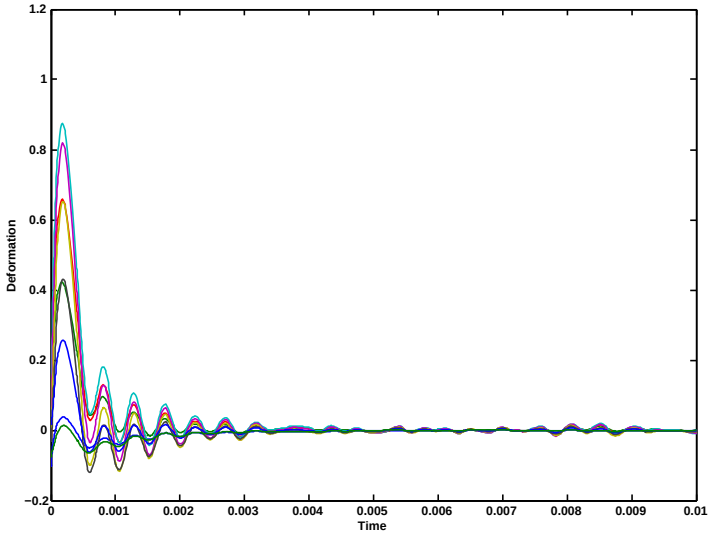

Figure 3.4: Response of the feedback loop under standard conditions. Deformation axis is scale to millimeters.

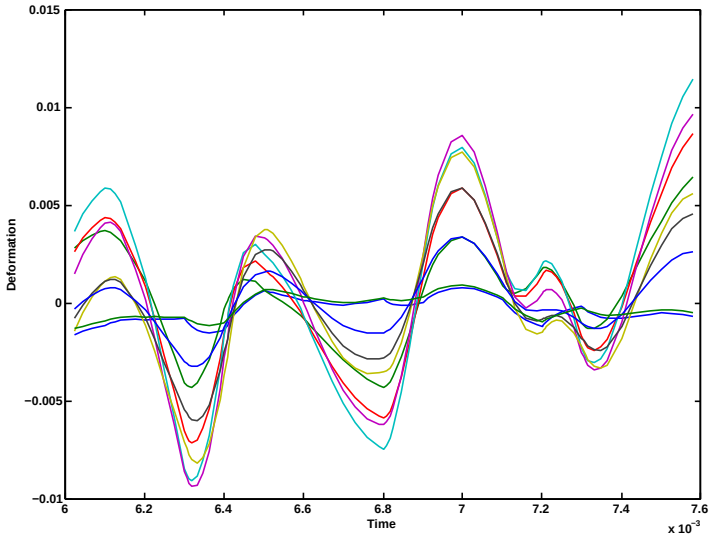

Figure 3.5: Steady state response of the feedback loop for *push-up* configuration.

was designed according to the procedure of IMC (Inverse Model Controller) explained in (1).

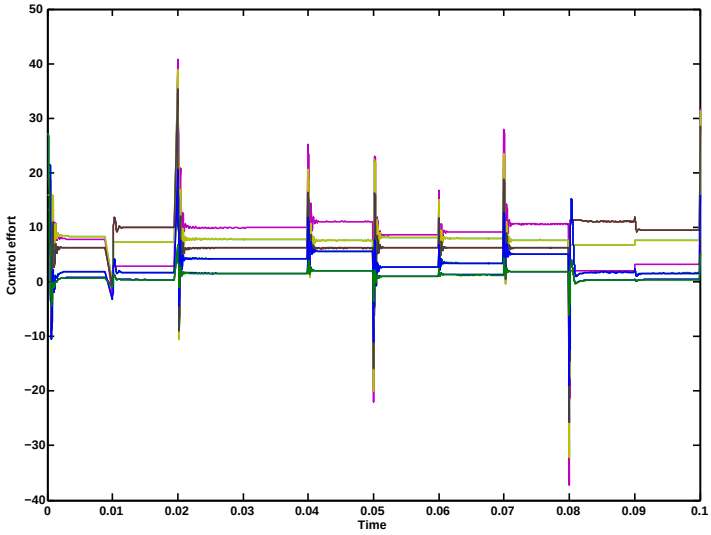

Figure 3.6: Control effort of the PI controller

Coming back to the nominal performance of this controller it is easy to see that it performs "good". Never the less in the sense of tracking the inputs when a disturbance is present it behaves not as it would be expected, this can be verified by inspection of the simulation showed in Figure 3.7 were it is notorious the difficulty that the controller faces to keep the output constant.

3.0.3 The *realistic* approach

Table 3.4 shows the eigenvalues of the plant in the *realistic* set of the piezo patch problem with dominant pole at -63.28 and acting under direct state noise influence, its deformation is showed in Figure 3.8.

A *LQG* controller is synthesized using parameters listed in Table 3.5 and the algorithm already described at the begging of the present chapter. This

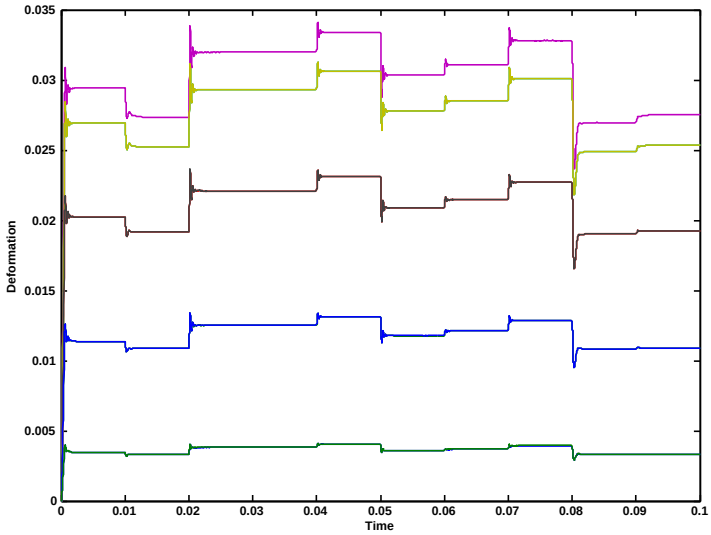

Figure 3.7: Response of the feedback loop of the PI controller.

Table 3.4: Eigenvalues of the plant for the *realistic* approach.

Plan Eigenvalues	
-1.2200e7	-1.1233e4
-1.0763e7	-8.8361e3
-7.3471e6	-4.0908e3
-1.7705e5	-2.1940e3
-8.9791e4	-9.3418e2
-4.3354e4	-4.9055e2
-1.9720e4	-8.5828e1
-1.5491e4	**-6.3280e1**

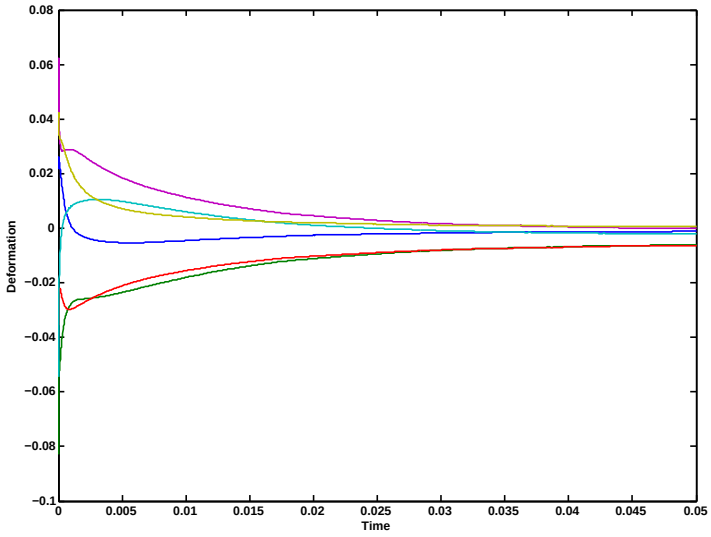

Figure 3.8: Plant response to state noise and random initial state.

time input criterium and state and measurement noises were more penalized in order to fulfill at the most the objectives listed in Section 2.4.1.lfil at the most the objectives listed in Section 2.4.1.

Table 3.5: Specifications for *realistic LQG* synthesis.

Weight on	**Value**
Q	1
R	1e-8
Xi	1e-8
Th	1e-8

Table 3.6 shows a list of the eigenvalues for the feedback system for standard conditions of state noise. One can see that in this design the dominant pole is located at -10.70 making the feedback system faster but resting an "amount" of robust performance against uncertainty, this can be also verified by inspection of the Figures 3.9 and 3.10.

One can see in figures 3.11 and 3.12 the behaivor of the damped rod under

Table 3.6: Eigenvalues for the controller-plant feedback on the *realistic* approach.

Feedback Eigenvalues			
-1.2223e7	-5.3120e5	-1.4337e4	-2.1940e3
-1.2200e7	-1.7705e5	-1.1702e4	-9.3418e2
-1.0788e7	-1.2020e5	-1.1233e4	-5.9748e2
-1.0763e7	-8.9791e4	-8.8361e3	-5.7873e2
-7.3659e6	-4.3354e4	-5.6825e3	-4.9055e2
-7.3471e6	-2.0049e4	-4.8907e3	-4.4887e2
-6.5883e5	-1.9720e4	-4.5761e3	-8.5828e1
-6.3197e5	-1.5491e4	-4.0908e3	**-1.0708e+001**

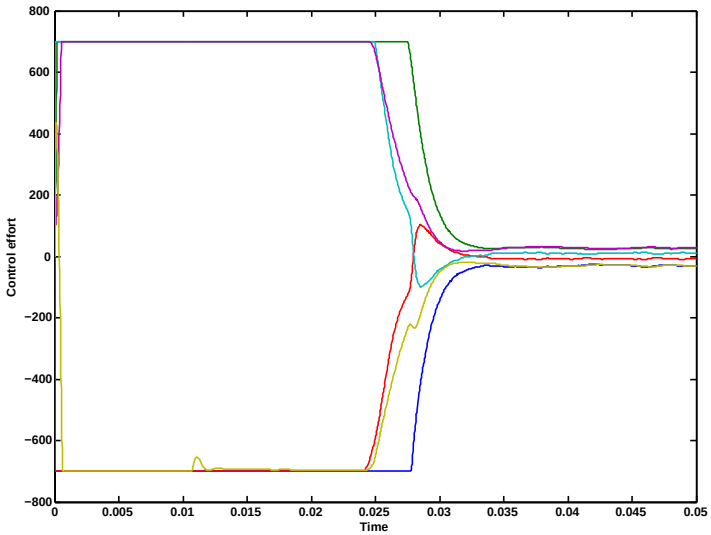

Figure 3.9: Control effort of the *LQG* controller for the *realistic* approach. One can notice that the actuators saturates at $700N$ even when the data sheet set it at $775N$ it was chosen this manner to give the design a security factor.

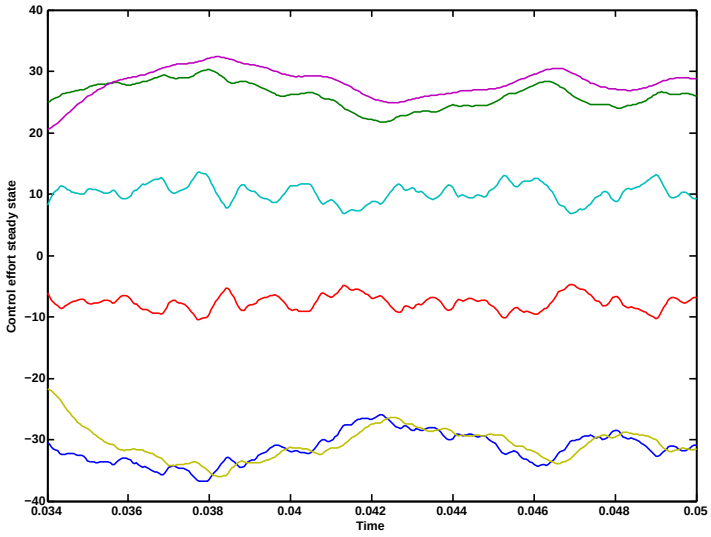

Figure 3.10: Steady state of the control effort for the *realistic* setting.

feedback control. At the last Figure, at steady state, the deformation is not completely avoided. In contrast with the efficient response of the controller in terms of a "quick" response that seems to counteract, in some way, the vibrational force. This can be verified by meaning of an inspection of the pair of figures 3.12 and 3.10.

3.0.4 Virtual Reality Model

For visualization of the simulations performed in MATLAB a virtual reallity model was build using the same name's toolbox. The model, see Figure 3.13, consist in 6 or 9 outputs depending on the analysis. Each output is supposed to be a section of the rod itself and its displacement the displacement of the selected point of the rod caused by the feedback control loop.

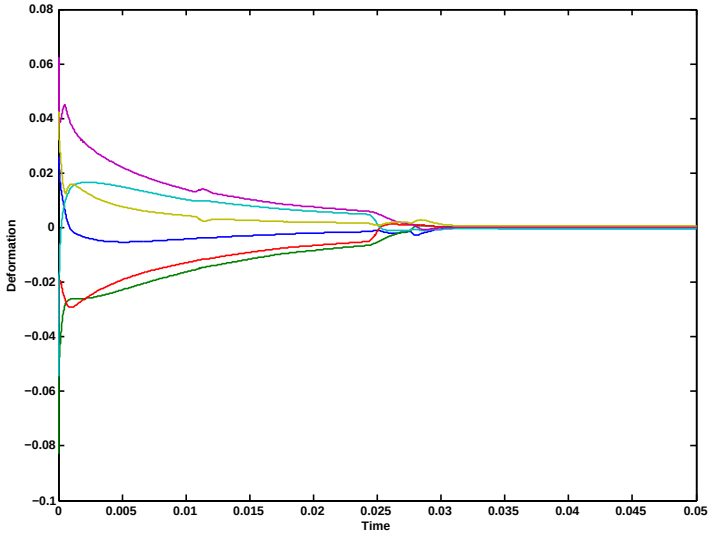

Figure 3.11: Deformation under feedback action of the *LQG* controller for the *realistic* approach. It could be interesting to set a comparison of the present Figure and 3.8.

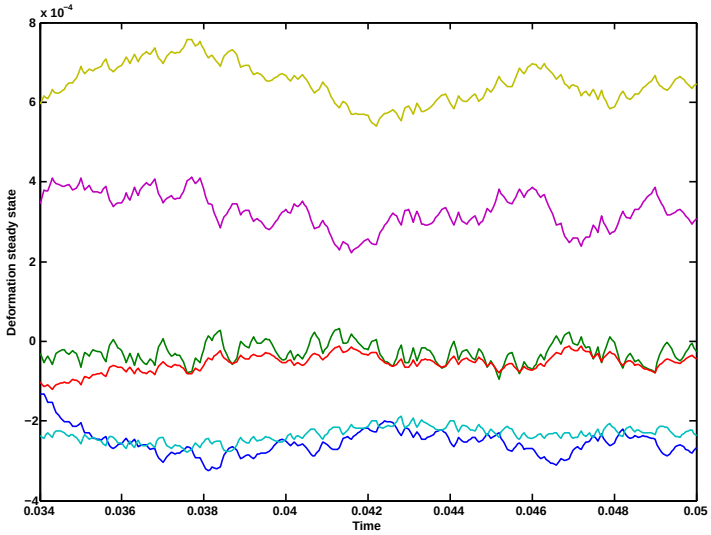

Figure 3.12: Steady state of the deformation under feedback control loop.

Figure 3.13: The 6 points VR model for the *realistic* setting performing a *strange* during a simulation.

Chapter 4

Summary and Conclusions

In the framework of disturbance rejection a *LQG* control approach has been presented for the active damping of vibrational disturbances on a rod of two different materials also, under, two different approaches of actuator configuration. Selection of a suitable set of piezo actuators and perifericals for the implementation of the system is also exposed. Model generation based in *FEM* is as well addressed.

From the simulations performed of the models treated in the present we can see that:

- The plant is highly interactive.
- Robust performance (one can almost be sure) is not satisfied for any of the designs, due to the fact that uncertainty was not explicitly taken in account while designing.
- Almost all, with the exception of the PI controller, the designs accomplish, until certain degree, nominal performance in the sense of satisfying the primary objective of the present.

It was seen during the whole analysis that saturation of actuators are an issue to concider as well as the high frequencies at which these most work. This was the primary reason to "eliminate" the *push-up* approach for further analysis and developement, it is just not real, and creates a "fake" impression of the control performance.

As one of the many ideas that are behind this work is to develop a control device that is capable of damping the vibration on the surface of a lent (adaptive optics) the *LQG* approach for the *realistic* setting is prefered over the other designs due that it provides a fast and "effective" control of vibration, in space normally one do not have a lot of time to take pictures and time is an compromise of the control system.

Even when there are some inaccuracies in the present such as model uncertainties that limits the analysis of the system one can think about mayor facts of concideration:

- Feedback system in the *push-up* approach has robust peformance in the sense of that it has a good disturbance rejection at the cost of a high frequency control response that no-transducer based on piezo electric principes can achive.
- Feedback system at steady state in the *realistic* approach, makes a compromise between the magnitud of deformation that is "kept" and the time that takes to damp the disturbance.

4.0.5 Future Work

One can think about different control configurations for this problem. One of them could be the design of a spatially decentralized control or, another way to go, could be to develop an H_∞ controller with the aim of include a

more detailed model of uncertainty and eventually synthesize a μ optimal controller.

One issue that must be take in account for future work is defenetly to include a more accurate and detailed model of disturbance in the analysis by means of including i.e. the closed loop disturbance gain matrix (CLDG). This can also help to understand better the dynamics and to be able to take decisions and attack the problem in a better way.

An analysis of robust performance with respect to input uncertainty could have been interesting, for this we need to stablish a maximum uncertainty possible as a function of the desired steady state accuracy.

It also would be interesting the dimensional *expantion* of the present work, by means of developing a control configuration for a 2D array of piezo actuators and sensors.

References

[1] K. J. Astrom. *Computer Controlled Systems.* Prentince-Hall, Inc., New Jersey, 1st, edition, 1984.

[2] S. J.M., B. J.C., S. I.S., and A. S. Piezo patch sensor/actuator control of the vibrations of a cantilever under axial load. *Elsevier Ltd*, Composite Structures(62):423–428, 2003.

[3] V. Kucera. The h2 control problem: State-space and transfer-function solutions. *Control and Automation, 2006. MED '06. 14th Mediterranean Conference on*, pages 1–5, June 2006.

[4] P. T. PI. Duraact piezoelectric patch transducers for industry and research, 2008. [Online; accessed 18-May-2008].

[5] S. Skogestad and I. Postlethwaite. *Multivariable Feedback Control. Analysis and Design.* John Wiley and Sons, Ltd., England, 2nd, edition, 2005.

Appendix A

MATLAB Code for *LQG* synthesis

```
disp(' ');
sys = input(' ***** LQG synt ***** n');
disp(' ');
sys = input(' Select a plant (form workspace) n ');
disp(' ');
ws = input(' Select a weight for the state criterum n ');
disp(' ');
wi = input(' Select a weight for the input criterum n ');
disp(' ');
wsn = input(' Select a weight for the state noise n ');
disp(' ');
wyn = input(' Select a weight for the output noise n ');
disp(' ');

rw,cl
=size(sys.b);
```

pesos del criterio JLQG

Q=ws*eye(rw);

R=wi*eye(cl);

W=[Q zeros(rw,cl); zeros(cl,rw) R];

Xi=wsn*eye(rw);

Th=wyn*eye(cl);

V=[Xi zeros(rw,cl); zeros(cl,rw) Th];

my$_lqg = lqg(sys, W, V)$;